Effects of External PIM Sources on Antenna PIM Measurements

Jin Tae Kim, In-Kui Cho, Myung Yung Jeong, and Tae-Goo Choy

Antenna Passive Intermodulation (PIM) level measurement results are rarely credited to be due to external signal receiving characteristics of the antennas or serious effects from external PIM sources, such as the anechoic chamber absorber and antenna tower. This paper presents an antenna PIM model for a reflected PIM measurement method. Based on the findings of null point generation and the behavior of the third order PIM values obtained by theoretical predictions and experimental results, we concluded that the results of the antenna PIM level test were influenced by the external PIM sources generated by the anechoic chamber absorber and the path differences of PIM signals coming into the antenna.

Manuscript received Nov. 3, 2001; revised Sept. 12, 2002.

Jin Tae Kim (phone: +82 42 860 6005, e-mail: myjinny@etri.re.kr), In-Kui Cho (e-mail: cho303@etri.re.kr), Myung Yung Jeong (e-mail: myjeong@etri.re.kr), and Tae-Goo Choy (e-mail: tgchoy@etri.re.kr) are with Basic Research Laboratory, ETRI, Daejeon, Korea.

I. INTRODUCTION

To satisfy the demand for large-capacity, high-speed wireless multimedia telecommunication services, multiple access schemes have been developed [1], [2]. However, because of the origin characteristics of radio frequency use, traffic congestion and limitations on radio spectrums increased the possibility of interference and resulted in degradation of service quality.

Passive Intermodulation (PIM) caused by the non-linearity characteristics of radio frequency (RF) passive devices, such as non-linear metal contacts or non-linear magnetic hysteresis of ferromagnetic materials, can cause serious radio interference. In frequency division diplexing (FDD) systems, where the transmit and receive systems are collocated, PIM from the transmit system can cause PIM distortion of original data signals if the PIM frequency is equal to the receiving frequency [3]. Many researchers have studied this with a view to controlling and minimizing the PIM generated by RF passive devices and have developed accurate PIM level measurement methods [4]-[6].

Non-radiative RF passive devices, such as cable-connector assemblies, RF connectors, and filters, are rarely affected by external electromagnetic waves, but radiative RF devices, especially antennas, are influenced seriously by external electromagnetic signals because of the receiving characteristics of RF signals. Therefore, antenna PIM level measurements require a specific isolated measuring environment, for example, an anechoic chamber.

Although anechoic chambers can provide an accurate and credible environment for PIM testing, electromagnetic absorbers used in such chambers have various reflection and scattering coefficient characteristics according to the applied

frequency band and antenna location in the chamber [7]. Moreover, pyramid absorbers used for lower reflectivity have thin ferrite tiles whose magnetic, non-linear hysteresis can cause PIM generation.

Thus, if PIM testing is conducted in an imperfect environment, the results can indicate the level of radio interference between the radiating electromagnetic signals from the antenna and the external environment surrounding the test antenna, rather than the antenna PIM level itself. In addition, this situation can reduce the credibility and reproducibility of the antenna PIM level measurements.

Our investigation surveyed the PIM generation sources in an antenna PIM measurement setup, with the antennas in close proximity, and compared two antenna PIM test methods, the reflected method and the forward method. From the information on the sources of the PIM generation, we developed a PIM model for antenna PIM testing in an anechoic chamber. Performing an antenna PIM level measurement on a commercially available sector antenna, we compared theoretical PIM predictions with our experimental results. This paper describes our investigation and discusses in detail the influences of an anechoic chamber environment on the antenna PIM test.

II. MEASUREMENTS OF THE ANTENNA PIM

1. PIM Sources in the Antenna

Similar to the intermodulation produced by active devices, PIM is generated when two or more RF signals pass through RF passive devices having non-linear characteristics [8], [9]. Generally the non-linearities of RF passive devices consist of contact non-linearity and material non-linearity. Contact non-linearity refers to all metal contact non-linearities causing non-linear current-voltage behavior, such as a tunneling effect, micro-discharge, and contact resistance. Material non-linearity refers to the bulk material itself. Magneto-resistivity of the transmission line, thermal resistivity, and non-linear hysteresis of ferromagnetic material are good examples. PIM generation in RF passive devices is caused by the simultaneous appearance of these PIM sources, and the macroscopic result is often dominated by one principal PIM source.

In the case of antennas, PIM is generated not only by the same PIM sources as in general RF passive components but also by the external test environment, such as the absorbers in the chamber and conducting metal materials. Since antennas are very sensitive to external electromagnetic waves, antenna PIM test results are seriously affected, unless the antenna is isolated completely, or radiated electromagnetic waves are absorbed perfectly by the absorbers of the anechoic chamber.

Pyramid absorbers with a ferrite tile or carbon fiber are excellent PIM generators because of their non-linear permeability and resistivity. Interactions between the two RF signals f_1 and f_2 and the absorber's non-linear characteristics create PIM signals, $f_{im} = mf_1 \pm nf_2$. If scattered or reflected PIM signals from the absorber are received by the antenna being tested, they interfere with the PIM level of the test antenna. Previous studies reported similar results: [10] was concerned with determining the practical efficiency of antenna tower components related to PIM characteristics and [11] with the electromagnetic wave scattering problems in satellite communication.

2. Antenna PIM Test Methods

PIM signals generated in RF passive devices have bi-directional travel, so PIM level testing for a reciprocal two-ports RF device can be performed by both the reflected method and the forward method [12]. The former detects the reflected PIM signal level from the DUT and the latter detects the throughput PIM level of the DUT. These two test methods can be applied to antenna PIM measurement system configurations (Fig. 1).

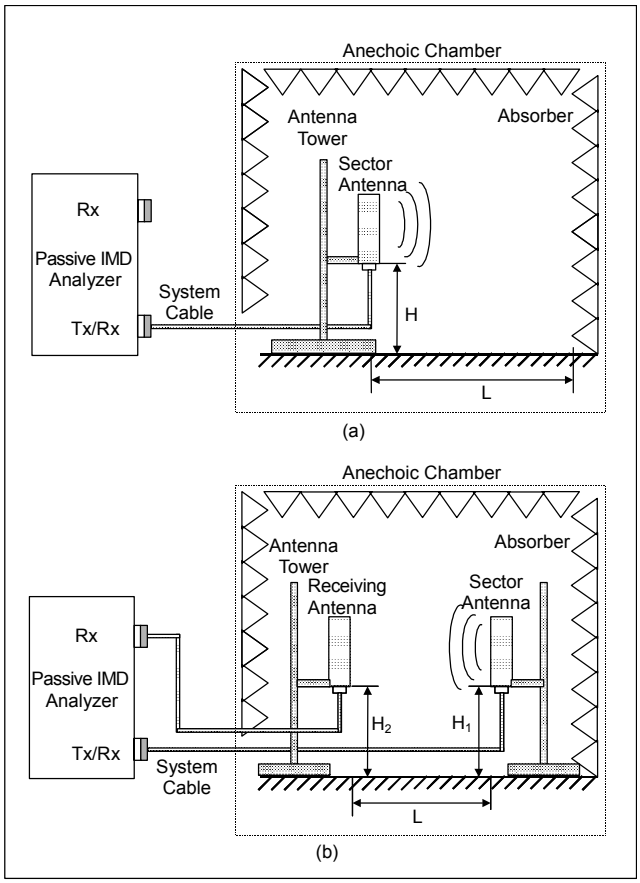

Fig. 1. Antenna PIM measurement set-up: (a) Reflected method, (b) Forward method.

Figure 1(a) describes the reflected method setup. As mentioned above, this method detects the reflected PIM signal from the test antenna, but there is a large probability that a scattered and reflected electromagnetic field will interfere with the actual antenna PIM level measurement, depending on how complete the absorber's absorbability is. Therefore, the reflective method should be made using more careful testing procedures and swept input frequency carriers with a sufficient sweep range to ensure that the maximum PIM level is found.

The forward method described in Fig. 1(b) detects radiating PIM signals from the test antenna, however the results were not reliable. There were not only the environmental interference problems experienced in the reflected method, but also qualification problems of the measurement equipment in the receiving part of the forward method. To measure radiating PIM signals from the test antenna, a low PIM antenna on the receiver side of the measuring setup is required and its PIM level should be qualified. However, there was no standardized examination of the antenna's qualifications. The PIM level qualification of the receiving antenna could be performed by the reflected method, but the results were also unreliable. Thus, enhancement of the reliability of the results for the reflected method is required. Moreover, more profound studies on antenna PIM level measurement are required.

3. Practical Antenna PIM Testing

Of the two PIM testing setups, the reflected method is more essential than the other because it can qualify a receiving antenna PIM level used in the forward method. Therefore, the reflected method was chosen for the first PIM test and modeling for the antenna PIM.

Practical antenna PIM level measurements were performed under the following environmental conditions: The anechoic chamber, which was used as a free-space environment, was designed for 3 m/10 m range electromagnetic interference measurements and consisted of pyramidal absorbers with a height of 1.72 m and a 0.60 m peak edge distance. The distance between the antenna and the pyramid absorber was 5 m. A Summitek Instruments SI-900A PIM analyzer with two-tone PIM test capability and each with output power at 43 dBm was used for PIM level detection.

The Tx frequency band of the global system for a mobile (GSM) system was swept from 935 MHz to 960 MHz, while each end of the range was fixed to make the third order PIM frequency range from 910 MHz to 915 MHz. Although the third order PIM signals made in the Tx band were in the 910 to 960 MHz range ($f_{im} = 2f_1 - f_2$) or 935 to 985 MHz range ($f_{im} = 2f_2 - f_1$), the third order frequencies produced outside the Rx band of the GSM system were not relevant, because the Rx band of the GSM system ranges from 890 MHz to 915 MHz. Therefore, the antenna PIM level measurements were performed in a range from 910 MHz to 915 MHz, while 935 MHz was fixed and the other frequencies were swept from 960 MHz to 955 MHz by steps of 0.5 MHz. The test antenna was a sector antenna; its specifications are shown in Table 1.

Table 1. Characteristics of the test antenna.

Frequency Range	890–960 MHz
Gain	15 dBi
Polarization	Vertical
Horizontal Beam Width (at 3 dB point)	65 °
Vertical Beam Width (at 3 dB point)	16 °
Front to Back Ratio	30 dB
VSWR	< 1.5
Isolation	> 30 dB
Height	1.2 m
Width	0.3 m

The residual PIM level of the analyzer with a low PIM 50 Ω termination was –163 dBc and did not show any results. We made the antenna PIM level measurements for different antenna heights from the floor.

The third order PIM frequency responses of the test antenna show a conspicuously low PIM level at a specific third order PIM frequency (Fig. 2). This is called the null point of the PIM

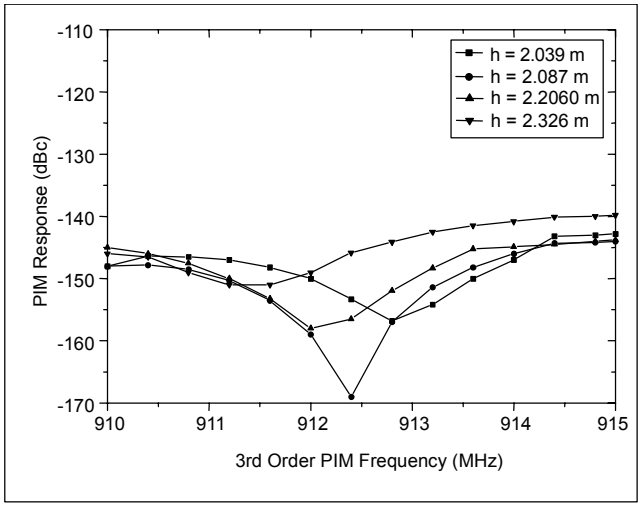

Fig. 2. The third order PIM frequency responses of the test antenna for different antenna heights.

frequency response; it moved to a lower third order PIM frequency with an increase in the height of the test antenna. Null point generation means that an RF system under the PIM test has many PIM sources, at least more than two, and their values are similar. If these PIM signals have a phase difference in the propagation vector, their combination results in null point generation at a specific frequency, and it is a function of both frequency and the electrical path length [13].

Figure 3 shows the null point changing in frequency according to the antenna height. It changed gradually to a lower PIM frequency with an increasing antenna height and was periodic. Its repetition was approximately equal to the interval of the absorber's vertexes.

In conclusion, the antenna PIM levels were influenced by an external interferer which caused periodicity in the results. The most probable external and periodic PIM sources were the incoming or scattered PIM signals from the pyramidal absorber. Incoming PIM signals were generated by the interaction between two radiated RF signals, f_1, f_2, and external non-linear sources. Scattered antenna PIM signals at the absorber could be received by the test antenna because it was designed for both transmit and receive frequency bands simultaneously.

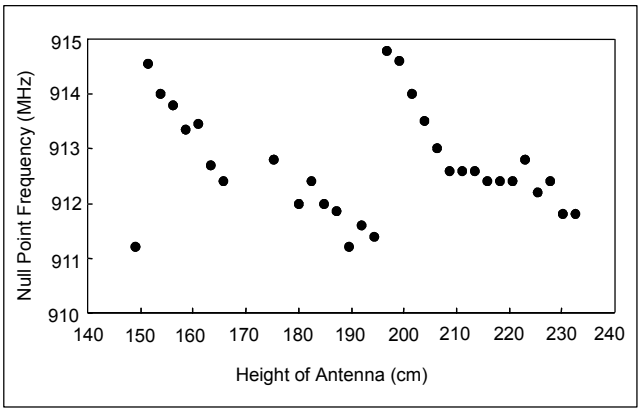

Fig. 3. The null point frequency shift versus the antenna height.

III. PIM MODEL OF THE ANTENNA

1. Theoretical PIM Model

We designed a theoretical PIM model to explain the experimental results of the antenna PIM behavior (Figs. 2 and 3). We constructed the antenna PIM model for the reflected PIM test method on the basis of the antenna PIM sources, as illustrated in Fig. 4.

Although there are many PIM sources in the antenna PIM test setup, dominant PIM sources determine the total PIM level of RF passive devices. In the reflected method setup for the

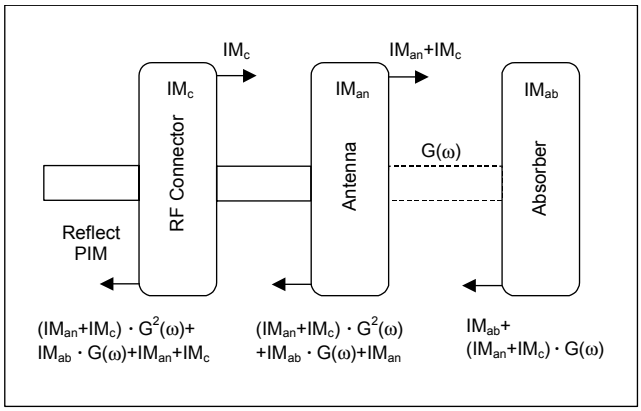

Fig. 4. Antenna PIM model for the reflected PIM test method.

antenna PIM testing, the dominant PIM sources can be represented by three components: the connector PIM generated between the antenna and the transmission line connection, the antenna PIM itself, and the absorber PIM.

Let the connector PIM level relative to the input signal be σ_c dBc. Its signal propagation is described as in [13],

$$IM_c = \sigma_c e^{j(2\omega_2-\omega_1)t} = \sigma_c e^{j\omega_3 t}, \tag{1}$$

where ω_3 is the third order PIM frequency in MHz. In the same way, the antenna PIM (IM_{an}) and the absorber PIM (IM_{ab}) can be written as

$$\begin{aligned} IM_{an} &= \sigma_{an} e^{j\omega_3 t} \\ IM_{ab} &= \sigma_{ab} e^{j\omega_3 t}. \end{aligned} \tag{2}$$

Because the total PIM level of one RF passive device is the summation of each PIM level, the reflected PIM level of the antenna is the summation of (1) and (2).

Electromagnetic signals passing through the RF cable take the same path, but incoming electromagnetic signals from the absorber take different paths depending on the point where scattering or PIM signal generation has occurred. Regarding this point, the group delay is introduced as follows:

$$G(\omega_3) = \sum_{i=1}^{n} e^{j\beta l_i}, \tag{3}$$

where Σ is a summation of every path, β is a wavenumber $2\pi/\lambda_3$, and l_i is an electrical length. As shown in Fig. 4, the radiated PIM signal from the antenna is $IM_c + IM_{an}$. This signal is scattered and reflected at the absorber and then returned to the test antenna again. The reflected PIM level from the antenna IM_{refG} is written as

$$IM_{refG} = (IM_c + IM_{an}) \cdot G^2(\omega_3). \quad (4)$$

Since the PIM signal generated in the absorber undergoes a group delay, it can be written as

$$IM_{abG} = IM_{ab} \cdot G(\omega_3). \quad (5)$$

The incoming PIM signals to the test antenna are $IM_{refG} + IM_{abG}$. The total PIM signals received by the test antenna are combined with the connector PIM signal and the antenna PIM signal, so the detected PIM level in the PIM analyzer using the reflected method is written as

$$\begin{aligned} IM_{ref} &= (IM_c + IM_{an}) \cdot G^2(\omega_3) + IM_{ab} \cdot G(\omega_3) + IM_c + IM_{an} \\ &= \left[(\sigma_{an} + \sigma_c) \sum_{i=1}^{n} e^{2j\beta l_i} + \sigma_{ab} \sum_{i=1}^{n} e^{j\beta l_i} + \sigma_{an} + \sigma_c \right] e^{j\omega_3 t}. \end{aligned} \quad (6)$$

2. Analysis of the Antenna PIM Model

For the analysis of the antenna PIM model, (6) was simulated with the same measurement dimensions as described in section II. 3. Among the many points where scattering, reflection, and PIM generation occurred, the vertexes of the absorbers were chosen as the main points. The PIM signals from the front vertexes were considered important because other vertex PIM signals have a lower probability of being received by the test antenna than other vertex signals. According to the location of the vertex and the geometrical distances, such as the interval of the vertexes (0.6 m) and the space between the test antenna and the vertexes in a straight line (> 5.0 m), the PIM signals incoming to the test antenna have many different passing roots l_i, where the number of passing roots is determined by the beam width of the test antenna covering the front vertexes.

The test antenna had four dipoles equally spaced at 0.3 m. We calculated many PIM signal paths having different electrical lengths between the vertexes and the dipoles of the antenna. Because the PIM signals from the vertexes radiated diversely in all directions and the width of the antenna (0.3 m) was smaller than the interval of the vertexes (0.6 m), the vertex PIM signals, the largest portion of the vertex PIM signals that were received by the test antenna, were the ones that had the shortest distance between the vertexes and the test antenna. Thus, the closer the vertexes were to the test antenna, the higher the probability of the PIM signals being received by the test antenna. If longer paths, which had a low possibility of being received, were negligible and the same values were deleted, the four shortest electrical paths remained, represented by l_1, l_2, l_3, and l_4, and with the reflected method they contributed to a larger extent to the total PIM level.

Figure 5 shows the PIM level dependency on the variation of the absorber's PIM level, where the connector and the antenna PIM levels were fixed at –150 dBc. When the absorber PIM levels were larger than those of the connector and the antenna, the PIM level showed high, stable values according to the PIM frequency. However, when the absorber PIM levels were smaller than the others, the PIM level was conspicuously low at a specific third order PIM frequency. This was similar to the experimental results (Fig. 2). This is called the null point of the PIM and it means that the external PIM levels are smaller than those of the test antenna.

The null point showed a deeper and more distinct shape as the PIM levels of the absorber decreased and then became saturated, if the PIM level difference between the absorber PIM level and two other PIM levels was more than 40 dBc. This prediction is opposite to the previous literature, which predicted no null point would be generated when the difference was more than 6 dBc [13].

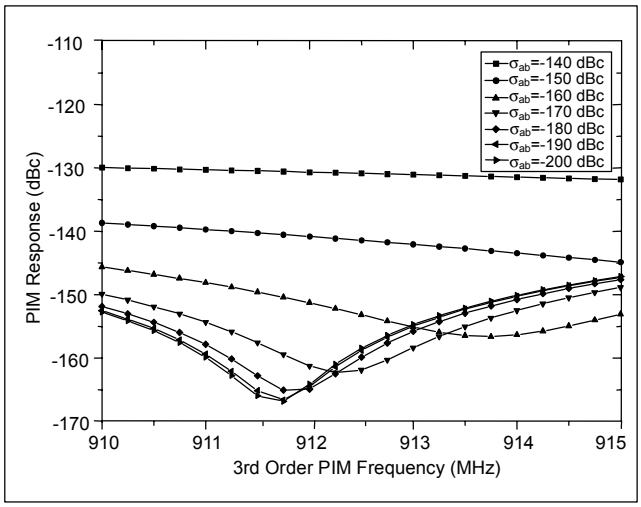

Fig. 5. Predicted PIM response with absorber PIM level variation ($\sigma_c = \sigma_{an}$ = –150 dBc).

Figure 6 shows the predicted PIM responses according to the variations of the connector and the antenna PIM levels when the absorber PIM level was fixed at –180 dBc. To simplify the parameters, the connector and the antenna PIM levels were assumed to be the same.

Because the absorber PIM level was much smaller than the two PIM sources, the null points were generated in a manner similar to the prediction (Fig. 5). The largest third order PIM responses were determined by the connector and the antenna PIM levels. When the absorber PIM level was equal to or larger than the other two, the null point disappeared and the maximum

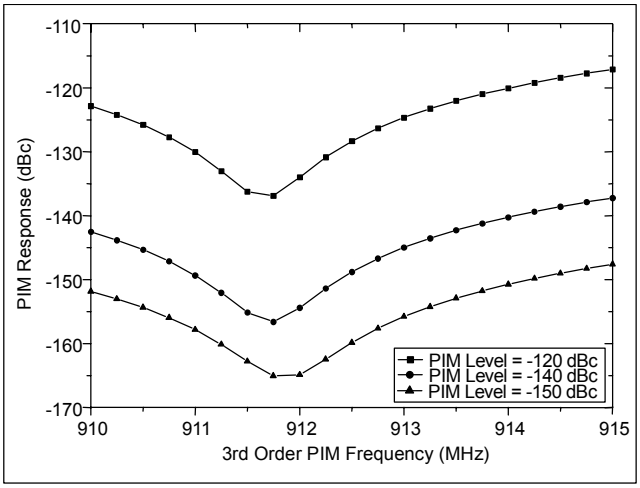

Fig. 6. Predicted PIM response with connector and antenna PIM level variation ($\sigma_{ab} = -180$ dBc, $\sigma_c = \sigma_{an}$).

PIM level was that of the higher value of the two PIM sources. When the connector and the antenna PIM levels were different, the highest third order PIM levels were also predicted to take a larger part in contributing to the total PIM level.

The path differences between the PIM signals from the vertexes of the pyramid absorbers created phase differences between them and affected the reflected PIM test results of the antenna. Figure 7 shows the predicted PIM responses with one arbitrary l_i variation. Although all the path lengths were changed according to the height variation of the test antenna, for simplicity, only one was considered for calculation. With a decrease in path l_i, the null point shifted to a lower PIM frequency and showed a sharper and deeper null point shape at a specific path length. PIM level variation according to the path

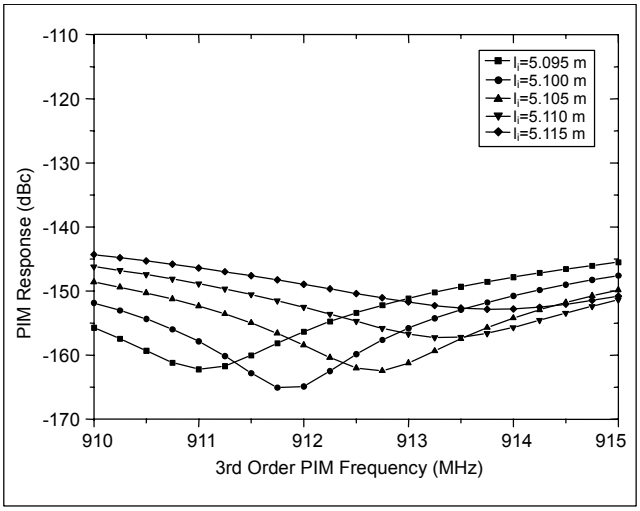

Fig. 7. Predicted PIM level behavior for different value of an arbitrary path length l_i.

difference means that the PIM level of the antenna is dependent on the antenna location in the anechoic chamber.

IV. DISCUSSION

Figure 8 shows the comparison between the experimental results and the theoretical predictions. The figure confirms that the predicted PIM responses and the actual measurement results are in good agreement. The null point of the third order PIM frequency and the maximum PIM level were the same. Moreover, the third order PIM pattern and the third order PIM frequency were nearly equal.

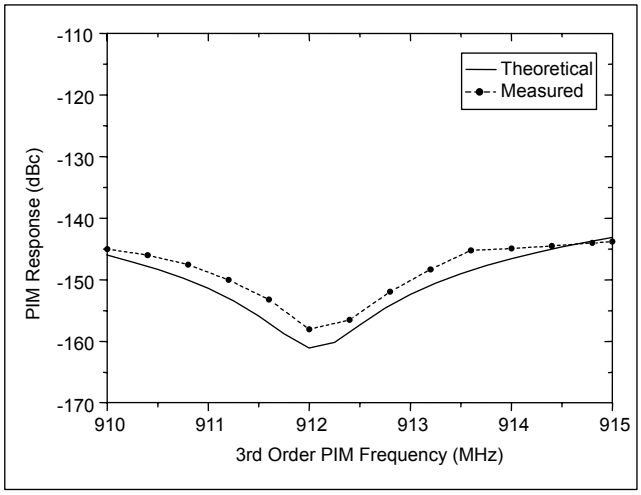

Fig. 8. Comparison between predicted and measured PIM results.

Since the total PIM signal is the result of the interaction between many diverse PIM sources, and the actual PIM levels of each of the pyramid absorbers were not equal in amplitude and path length, a small disagreement existed between the predicted and experimental PIM results.

When the connector and the antenna PIM levels were the same, the calculation was simpler, but it did not agree with the experimental PIM level pattern. The exact PIM level and pattern was obtained when the connector and the antenna PIM levels were different.

Considering the PIM levels of the connector and the antenna, when either one was higher than the other, the null point did not appear in the PIM level predictions. This phenomenon was revealed in the practical PIM level measurement with a high PIM antenna. This could be explained by the fact that a lower PIM signal was submerged in higher PIM signals and it did not influence the larger results.

In the case of the absorber, however, the null point was deeper and sharper when its PIM level was much smaller than that of the other PIM levels.

The maximum PIM level in Fig. 8 is –145 dBc at 43 dBm input RF power, and we considered it as the actual PIM level of the test antenna. In the theoretical calculation, the absorber PIM level was no more than –180 dBc.

V. CONCLUSION

From an antenna PIM level measurement using the reflected PIM testing method, we found that a null point occurred where the PIM level showed the lowest value at a specific third order PIM frequency.

We can explain the null point phenomenon as being caused by the influence of external PIM sources, such as the scattered and reflected PIM from the absorber and newly incoming PIM signals generated in the absorbers.

The third order PIM level behavior of the antenna was influenced by external PIM sources, such as the absorber PIM level and the propagation path length of the external PIM signal, rather than internal PIM sources, such as the connector PIM.

We conclude that to obtain the maximum PIM level, PIM testing of the antenna must always be made under conditions in which the effect from external PIM sources is minimized and a sufficiently large frequency sweep range is applied. Finally, for accurate antenna PIM evaluation, the measurement must be performed precisely.

REFERENCES

[1] Youngnam Han, Hang Gu Bahk, and Seungtaik Yang, "CDMA Mobile System Overview: Introduction, Background, and System Concepts," *ETRI J.*, vol. 19, no. 3, Oct. 1997, pp. 83-97.

[2] W.C.Y. Lee, *Mobile Cellular Telecommunications-Analog and Digital Systems*, 2nd Ed., McGraw Hill, 1995.

[3] P.L. Lui, "Passive Intermodulation Interference in Communication Systems," *Electronics & Communication Engineering J.*, vol. 2, June 1990, pp. 109-118.

[4] T. Khattab and A.D. Rawlins, "Principles of Low PIM Hardware Design," *Thirteenth National Radio Science Conf.*, 1996, pp. 355-362.

[5] G.H. Schennum and G. Rosati, "Minimizing Passive Intermodulation Product Generation in High Power Satellites," *IEEE Proc. of Aerospace Applications Conf.*, vol. 3, 1996, pp. 155-164.

[6] J.A. Jargon, D.C. DeGroot, and K.L. Reed, "NIST Passive Intermodulation Measurement Comparison for Wireless Base Station Equipment," 52*nd ARFTG Conf. Digest, Computer-Aided Design and Test for High-Speed Electronics*, 1998, pp. 128-139.

[7] C.L. Holloway et al., "Comparison of Electromagnetic Absorber Used in Anechoic and Semi-Anechoic Chambers for Emissions and Immunity Testing of Digital Devices," *IEEE Trans. Electromagnetic Compatibility*, vol. 39, 1997, pp. 33-47.

[8] B.G.M. Helme, "Passive Intermodulation of ICT Components," *IEE Colloquium on Screening Effectiveness Measurements*, 1998, pp. 1/1-1/8.

[9] P.L. Lui and A.D. Rawlins, "Passive Non-linearities in Antenna Systems," *IEE Colloquium on Passive Intermodulation Products in Antennas and Related Structures*, 1989, pp. 6/1-6/7.

[10] P.L. Lui and A.D. Rawlins, "The Field Measurement of Passive Intermodulation Products," *Fifth Int'l Conf. on Mobile Radio and Personal Communications*, 1989, pp. 199-203.

[11] P. Bolli et al., "A Time Domain Physical Optics Approach to Passive Intermodulaton Scattering Problems," *IEEE Int'l Symp. on Antennas and Propagation Society*, vol. 3, 1999, pp. 2018-2021.

[12] B. Rosenberger, "The Measurement of Intermodulation Products on Passive Components and Transmission Lines," *IEEE MTT-S Symp. on Technologies for Wireless Applications*, 1999, pp. 57-62.

[13] B. Deats and R. Hartman, "Measuring the Passive-IM Performance of RF Cable Assemblies," *Microwaves & RF*, Mar. 1997, pp. 108-114.

Jin Tae Kim received his BS degree in physics from University of Incheon in 1996 and his MS from Korea University in 1998. His main research was on NMR/MRI and he worked in Asan Medical Center, Seoul, Korea, in 2000. In October 2000, he joined Electronics and Telecommunications Research Institute (ETRI), Daejeon, Korea, where he worked on the Passive Intermodulation (PIM) in mobile telecommunication components. Since 2002, he has investigated a polymeric waveguide device based on LIGA, MEMS and hot embossing.

In-Kui Cho was born in Kyungnam, Korea, on April 8, 1970. He received the BS and MS degrees from Kyungpook National University, Korea in 1997 and 1999. Since May 1999, he has worked for Electronics and Telecommunications Research Institute (ETRI). Present research interests include Passive Intermodulation (PIM) of RF components, optical interconnection, and packaging.

Myung Yung Jeong was born in Kyungnam, Korea, on February 20, 1960. He received the BS and MS degrees from Pusan National University, Korea in 1982 and 1984, respectively, and the PhD degree from Korea Advanced Institute of Science and Technology, Korea in 2000. Since September 1983, he has worked for Electronics and Telecommunications Research Institute (ETRI). Present research interests include hot embossed optical devices, photonic crystals, optical interconnection and packaging. He is now the Team Leader of the Optical Interconnection Team, ETRI.

Tae-Goo Choy received the BS and MS degrees in physics from Korea University in 1972 and 1976, respectively. He joined the Component Technology Development Section at ETRI in 1977, where he is currently Head of Section. He is interested in microwave and optical components. He holds 15 patents and authored over 40 papers.